Atomic Bloch-Zener Oscillations and Stückelberg Interferometry in Optical Lattices

Sebastian Kling,* Tobias Salger, Christopher Grossert, and Martin Weitz

Institut für Angewandte Physik der Universität Bonn, Wegelerstrasse 8, 53115 Bonn, Germany

(Received 11 June 2010; revised manuscript received 21 September 2010; published 16 November 2010)

We report on experiments investigating quantum transport and band interferometry of an atomic Bose-Einstein condensate in an optical lattice with a two-band miniband structure, realized with a Fourier-synthesized optical lattice potential. Bloch-Zener oscillations, the coherent superposition of Bloch oscillations and Landau-Zener tunneling between the two bands, are observed. When the relative phase between paths in different bands is varied, an interference signal is observed, demonstrating the coherence of the dynamics in the miniband system. Measured fringe patterns of this Stückelberg interferometer allow us to interferometrically map out the band structure of the optical lattice over the full Brillouin zone.

DOI: 10.1103/PhysRevLett.105.215301 PACS numbers: 67.85.Hj, 03.75.Dg, 05.60.Gg, 37.10.Jk

The transport properties of a quantum object in a periodic potential are crucially determined by the particle's band structure [1]. For example, Bloch oscillations, in which a particle subjected to a uniform force in a periodic potential performs an oscillatory rather than a uniformly accelerated motion, can be well described by the dynamics within a single band of the Bloch spectrum [2,3]. For systems with two bands energetically separated from energetic higher bands (miniband structure), as can be realized by imposing a superlattice structure onto a usual sinusoidal lattice potential, Bloch-Zener oscillations, a characteristic sequence of Bloch oscillations and Landau-Zener transitions, have been predicted to occur when a constant force is applied [4,5]. Experimentally, Bloch-Zener oscillations have been observed for light waves in waveguide arrays, while the phase coherence between interfering path has not been explicitly verified [6]. Interestingly, in Bloch-Zener oscillations the avoided crossing between the two minibands acts as a coherent beam splitter, where partial Landau-Zener tunneling between the subbands occurs. Since the avoided crossing is used here first to coherently split up and subsequently to recombine atomic wave packets, we expect to be able to observe an interference pattern, when the phase between the path in the two different subbands is varied. This is analogous to the Stückelberg oscillations long known in collisional atomic physics [7–9], and the corresponding fringe signal offers the possibility to interferometrically map out the band structure of the optical lattice.

Stückelberg interference based on two partial Landau-Zener transitions has been observed with Rydberg atoms [10], superconducting systems [11,12], and in ultracold molecular physics where this method was applied to measure Feshbach molecular levels [13]. For cold atoms in optical lattices, vibrational frequencies and the splitting between bands at the position of the gaps can be readily determined by the well-established techniques of parametric heating [14], Rabi oscillations at the gaps [15], and Landau-Zener tunneling [16]. The full band structure of an optical lattice can be determined by Bragg spectroscopy [17], but this requires a continuous change of the angle between the driving laser beams [18].

Here we report on the observation of Bloch-Zener oscillations with ultracold atoms in an optical lattice, as a generalization of the celebrated Bloch oscillations for a system with a two-band miniband structure. We have also observed an interference signal based on two partial Landau-Zener transitions between Bloch bands of the optical lattice. From measured fringe patterns of this Stückelberg interferometer, the energetic splitting between the bands at an arbitrary value of the atomic quasimomentum can be determined. Thus, a novel method is realized to interferometrically map out the band structure of an optical lattice *in situ*.

Our experiment uses lattice potentials realized by superimposing a conventional standing wave lattice potential of $\lambda/2$ spatial periodicity with a $\lambda/4$ periodicity lattice realized with the dispersion of a multiphoton Raman process [19,20]. The splitting between the lowest energetic Bloch band and the first excited band is determined by first order Bragg scattering of the standing wave lattice potential, while the splitting between the first and the second excited bands is due to the interference of contributions of second order Bragg scattering of the standing wave lattice potential and of first order Bragg scattering of the fourth order ($\lambda/4$-spatial periodicity) lattice. By choosing a relatively large value of the amplitude of the multiphoton lattice potential, the splitting between the first and the second excited bands can be made large so that the tunneling rate to higher bands is small. In this way, a miniband structure with two closely spaced subbands is prepared, where in between the Landau-Zener tunneling rate is large. In the following, V_1 and V_2 denote the potential depths of the two lattice harmonics with spatial periodicities $\lambda/2$ and $\lambda/4$, respectively, ϕ is the relative phase between lattice harmonics, and $k = 2\pi/\lambda$ is the optical wave vector. The Fourier-synthesized lattice potential reads $V(z) = (V_1/2)\cos(2kz) + (V_2/2)\cos(4kz + \phi)$. If Δ_1 and Δ_2

denote the splittings between the ground and the first excited band, and the first and the second excited bands, respectively [see Fig. 1(a)], Δ_2 is maximized for a relative phase between lattice harmonics of $\phi = 0$, because the contributions from both lattice harmonics to this splitting then interfere constructively [20]. If $\Delta_2 > \Delta_1$, as is desirable when considering atom dynamics in the lowest two bands, the corresponding bands are commonly called minibands. In general, minibands emerge above a certain value of the ratio of the potential depth of the harmonics: $V_2/V_1 > r(\phi, V_1, V_2)$. Figure 1(a) shows the calculated band structure of such a lattice for the experimental parameters used.

Our experiment starts with an atomic rubidium Bose-Einstein condensate loaded into a lattice at rest relative to the rest frame of the atoms, so that atoms are transferred into the lowest energy band at a quasimomentum $q(0) = 0$. Subsequently, the lattice is accelerated relative to the free-falling atoms, which is equivalent to the application of an external force F to the atoms, and the quasimomentum evolves in time to larger quasimomenta, following $q(t) = q(0) + F \cdot t$. By the time the atomic wave packet reaches the first band gap, part of the wave packet experiences Landau-Zener tunneling through the gap into the first excited Bloch band, while the remaining part remains in the lowest band and is Bragg reflected. The corresponding beam splitting process is visualized in the extended band structure scheme shown in Fig. 1(a). The splitting ratio can be controlled by tuning the size of the gap, which to lowest order is determined by the magnitude of V_1. In this way, a coherent superposition of wave packets in the two different subbands of the miniband structure is created. To shift the relative phase between the two paths, the acceleration can be stopped at some value of the quasimomentum q_0 [with $q_0 = q(t_0)$ and $\hbar k \leq q_0 \leq 3\hbar k$] for a waiting time t_w. We expect that the wave functions during this waiting time in the two bands then evolve as (with $t_0 \leq t \leq t_0 + t_w$)

$$\psi_j(t) = \psi_j(t_0) \exp[-iE_j(q_0)(t - t_0)/\hbar], \qquad (1)$$

where $j = 1$ for the lowest band and $j = 2$ for the first excited band, respectively; $E_1(q_0)$ and $E_2(q_0)$ denote the corresponding eigenenergies at a quasimomentum q_0. In a waiting time t_w, a relative phase between the bands $\Delta\varphi = [E_2(q_0) - E_1(q_0)]t_w/\hbar$ is accumulated. Subsequently, the acceleration is continued, and at a quasimomentum of $3\hbar k$ in the extended band scheme of Fig. 1(a), we again reach the band gap between the ground and the first excited Bloch band, where Landau-Zener tunneling acts as a second beam splitter to recombine the two wave packets and close the atom interferometer. The acceleration stops here at a quasimomentum of $3\hbar k$ and the lattice is switched off, after which a time of flight image is recorded. Correspondingly, the lattice eigenstates at the position of the crossing are mapped onto the free atomic eigenstates.

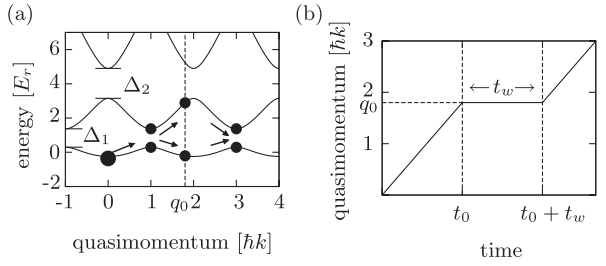

FIG. 1. (a) Band structure of the Fourier-synthesized optical lattice potential along with the scheme of the Stückelberg interferometer. The parameters used for the band structure were $V_1 = 2.7E_r$, $V_2 = 3.2E_r$, and $\phi = 0°$. (b) Variation of the quasimomentum with time for realizing the Stückelberg interferometer.

Depending on the relative phase between wave packets, atoms at the interferometer output will either be transferred into the first or the second diffraction order in the far field image. As a function of the waiting time t_w in the acceleration sequence, we expect a sinusoidal fringe pattern oscillating between the two different lattice diffraction orders. Notably, as this fringe pattern oscillates at a frequency $\omega = [E_2(q_0) - E_1(q_0)]/\hbar$, the oscillation frequency allows us to interferometrically determine the energetic splitting between the ground and the first excited band of the Bloch spectrum at a given value of the quasimomentum q_0. Figure 1(b) shows a scheme of the variation of the lattice quasimomentum with time. It is clear that from a variation of the quasimomentum at which the acceleration is stopped, the complete spectrum $\omega(q)$ of the miniband structure can be mapped out. We expect that this description is valid when the Landau-Zener tunneling rate into higher bands is small, as can be achieved for gap sizes $\Delta_2 > \Delta_1$ in the miniband structure. Otherwise, we expect a reduced number of atoms at the interferometer output due to loss into other diffraction orders.

Bloch-Zener oscillations now refer to measurements where the relative phase between the two wave packets is left at a constant value, as can be reached by simply setting $t_w = 0$ (i.e. omitting the waiting time) and monitoring the populations in the different bands versus time. In this case, we expect that the mean atomic momentum performs a characteristic double periodic motion with the two Bloch periods $T_B^{(1)} = 2\hbar k/F$ and $T_B^{(2)} = 4\hbar k/F$ [4]. This corresponds to a coherent superposition of Bloch oscillations and Landau-Zener tunneling in the two-miniband structure.

The experimental setup we used to investigate ultracold rubidium atoms in a Fourier-synthesized optical lattice is similar to the one described previously in Ref. [21]. An atomic rubidium (^{87}Rb) Bose-Einstein condensate is produced by evaporative cooling of atoms in a quasistatic optical dipole trap, after which the dipole trapping potential beam is extinguished, leaving the atoms in a ballistic free fall. The vertically oriented lattice beams are activated 2.5 ms after the release of the condensate from the trap, so that due to the lowering of the density during expansion, the interatomic interactions are reduced. The fundamental spatial frequency of spatial periodicity $\lambda/2$ of the

Fourier-synthesized lattice potential, with which the described miniband structure can be achieved, is created with a standing wave detuned by 1 nm to the red of the rubidium D_2 line. A lattice with spatial periodicity $\lambda/4$ is realized with the dispersion of Doppler sensitive four-photon Raman transitions between the ground state Zeeman sublevels, driven by the same laser. For more details, see the supplementary material [22]. During the free fall of the atoms, the lattice beams are initially switched on to adiabatically load the atoms into the lowest band of the Fourier-synthesized lattice at $q = 0$. For a measurement of Bloch-Zener oscillations, the lattice beam frequencies are acousto-optically shifted to accelerate the lattice with respect to the atoms' rest frame with a constant acceleration of 25 m/s^2 for the experimental data shown. The depths of the lattice harmonics were $V_1 = 2.7E_r$ and $V_2 = 3.2E_r$, where $E_r = (\hbar k)^2/2m$ denotes the recoil energy, and the relative phase between the harmonics was $\phi = 0°$.

Figure 2(a) shows the measured relative populations of the different diffraction orders of the lattice after a variable acceleration time t. The data allow us to follow the wave packet motion in the miniband Bloch band structure [see Fig. 1(a)] in time. When $F \cdot t \approx \hbar k$, the band gap between the ground and the first excited Bloch band is reached and the acceleration over this gap causes a first beam splitting process due to partial Landau-Zener tunneling. We observe a subsequent decrease of the population of the zeroth diffraction order (data with triangles) and an increase of the population of the first diffraction order to roughly 40% (filled circles). At the time when $F \cdot t \approx 2\hbar k$, the zeroth order peak is Bragg deflected into the second order peak (data with open squares); i.e., only the mapping onto the free eigenstates changes. When $F \cdot t \approx 3\hbar k$ is reached, a partial Landau-Zener transition occurs with the relative phase between wave packets for the data set shown being such that most of the population is transferred into the lowest energy band, which after the crossing maps onto the second diffraction order, and the observed corresponding relative population then increases to roughly 85%. The difference to 100% here is mainly due to partial Landau-Zener tunneling into higher bands (see the nonvanishing population of the zeroth order peak (triangles) at this time). For larger times, a second cycle of the wave packet motion in the miniband structure is observed. We attribute the corresponding data as evidence for Bloch-Zener oscillations in the Fourier-synthesized optical lattice. Figure 2(b) gives the mean velocity of the atoms in the coaccelerated frame versus time, as derived from the data of Fig. 2(a). We note that the relative phase between wave packets acquired during the sequence depends on the parameters of the lattice potential used (amplitudes of the harmonics and relative phase). When the splitting between the bands is varied so that a different phase is acquired between the partial Landau-Zener transitions, after the second splitting (for which $F \cdot t \approx 3\hbar k$) the population can, alternatively, also be mostly transferred into the first order peak, or partially into the first and second order peaks.

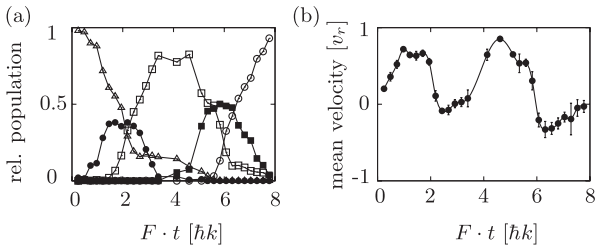

FIG. 2. Experimental data for Bloch-Zener oscillations of atoms in the biharmonic lattice potential, which was accelerated with a constant acceleration relative to the atomic rest frame. Here the quasimomentum $F \cdot t = 4\hbar k$ is reached after an acceleration time of $t = 955$ μs. (a) Relative population of diffraction orders versus time: zeroth order (triangles), first order (filled circles), second order (open squares), third order (filled squares), and fourth order (open circles), respectively. The solid line is to guide the eye. (b) Mean atomic velocity (circles) in the comoving frame versus time, where $v_r = \hbar k/m$ denotes the recoil velocity and m the atomic mass. The solid line is a spline fit.

Figure 3(a) shows data where the relative phase was varied between the two interfering paths of the formed Stückelberg band interferometer. For the corresponding measurement, the acceleration sequence was stopped after the first beam splitting process at a certain value of the quasimomentum q_0 (with $q_0 = 1.9\hbar k$ for the data shown here) for a variable waiting time to induce a variable phase shift. The filled (open) circles in Fig. 3(a) give the measured population in the first (second) order Bragg peak after releasing the condensate from the lattice when reaching a quasimomentum of $3\hbar k$. As a function of the waiting time t_w, which, due to the energy difference of the two bands, tunes the accumulated relative phase, a clear interference pattern in the relative population of Bloch bands is observed at the interferometer output. The observed interference signal of this Stückelberg interferometer was found to be very robust, as the additional variable waiting time t_w at a constant potential depth allows for a controlled tuning of the relative phase between the interfering arms of the interferometer for a broad set of experimental parameters. Let us point out that the Stückelberg interferometer may also be operated with two fully symmetric beam splitters when continuing the acceleration beyond the second beam splitter, i.e. for example, up to a quasimomentum of $3.5\hbar k$. A numerical simulation indicates that the expected fringe contrast for both cases is quite comparable.

From the measured oscillation frequency of the Stückelberg interference signal shown in Fig. 3(a), the energy difference between the Bloch bands at the corresponding quasimomentum can readily be determined. We attribute the observed damping of the fringe signal for large times t_w to the finite velocity spread of atoms after their release from the trap. By the time of the experiment, the condensate interaction energy has been converted into kinetic energy. The corresponding velocity spread is expected to cause a nonzero width of the quasimomentum distribution in the lattice. This will lead to a spread of

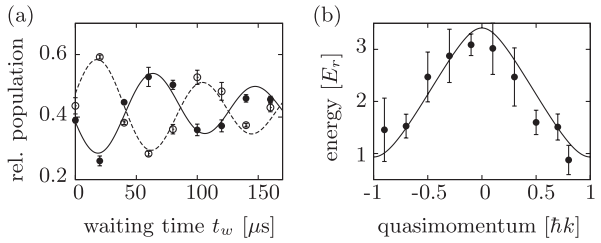

FIG. 3. (a) Measured Stückelberg interference fringes based on two partial Landau-Zener transitions between the band gaps of the optical lattice. The filled (open) circles give the measured relative population in the first (second) diffraction, respectively, versus the waiting time t_w, with $q_0 = 1.9\hbar k$ for this data set. The dashed and solid lines are fits to the data. (b) The data points give the interferometrically determined energy difference between the two minibands versus the lattice quasimomentum in the atomic frame. The solid line is the calculated energy difference.

oscillation frequencies of the Stückelberg interference signal, and a corresponding loss of contrast for larger times t_w. The solid and dashed lines in Fig. 3(a) are fits to the experimental fringe signal with a convolution of sinusoidal curves to account for the loss of contrast for larger times t_w (for a measured atomic velocity spread of $\pm 0.8\hbar k$ for this data set). We note that in a quantum simulation view of our two-band Bloch structure experiment, the observed oscillation frequency can be interpreted as a beating occurring at the ''quasirelativistic'' *Zitterbewegung* frequency [23,24]. Figure 3(b) shows the derived energy splitting between the ground and the first excited Bloch band of the miniband structure as a function of the quasimomentum for the complete Brillouin zone. The solid line is the theoretically expected curve of the energy difference for the given experimental parameters of the potential depths and relative phase of lattice harmonics, which is in good agreement with the corresponding experimental values. The smaller variation of the measured energy difference over the Brillouin zone with respect to the theoretical curve is attributed to the nonzero atomic velocity spread.

To conclude, we have observed Bloch-Zener oscillations in an optical lattice with a miniband-type Bloch band structure. The relative phase of wave packets in different Bloch bands was varied, which has allowed us to demonstrate the coherence of the formed Stückelberg interferometer and to demonstrate a novel method to interferometrically map out the energy difference between bands over the complete Brillouin zone.

We expect that the method described has prospects for precise interferometric determinations of the band structure in optical lattices. The velocity spread of the atoms can be reduced by Raman selection [25]. In principle, the method should also be applicable to usual standing wave lattices when, during the acceleration sequence, the Landau-Zener tunneling rate between Bloch bands is tailored dynamically either by appropriate variation of the potential depth of the lattice, similar to that described in [26], or by variation of the acceleration rate with time. For example, when the ramp speed is correspondingly reduced in the vicinity of the crossing between the first two excited bands, the tunneling rate to higher bands can be kept small. Other prospects for the discussed coherent manipulation in the miniband structure can include quantum simulations of the (linear and nonlinear) Dirac equation [24,27]. The interferometric method described may also be used to test for deviations of Newton's law over microscopic distances, in a spirit similar to earlier experiments based on Bloch oscillations [28].

We thank D. Witthaut for helpful discussions. Financial support from the DFG is acknowledged.

*kling@iap.uni-bonn.de

[1] See e.g. N. W. Ashcroft and N. D. Mermin, *Solid State Physics* (Saunders College Publishing, New York, 1976).
[2] J. Feldmann *et al.*, Phys. Rev. B **46**, 7252 (1992).
[3] M. Ben Dahan *et al.*, Phys. Rev. Lett. **76**, 4508 (1996).
[4] B. M. Breid, D. Witthaut, and H. J. Korsch, New J. Phys. **8**, 110 (2006).
[5] B. M. Breid, D. Witthaut, and H. J. Korsch, New J. Phys. **9**, 62 (2007).
[6] F. Dreisow *et al.*, Phys. Rev. Lett. **102**, 076802 (2009).
[7] E. C. G. Stückelberg, Helv. Phys. Acta **5**, 369 (1932).
[8] E. E. Nikitin and S. Y. Umanskii, *Theory of Slow Atomic Collisions* (Springer, Heidelberg, 1984).
[9] S. N. Shevchenko, S. Ashhab, and F. Nori, Phys. Rep. **492**, 1 (2010).
[10] S. Yoakum, L. Sirko, and P. M. Koch, Phys. Rev. Lett. **69**, 1919 (1992).
[11] W. D. Oliver *et al.*, Science **310**, 1653 (2005).
[12] M. Sillanpää *et al.*, Phys. Rev. Lett. **96**, 187002 (2006).
[13] M. Mark *et al.*, Phys. Rev. Lett. **99**, 113201 (2007).
[14] S. Friebel *et al.*, Phys. Rev. A **57**, R20 (1998).
[15] A. S. Mellish *et al.*, Phys. Rev. A **68**, 051601 (2003).
[16] O. Morsch and M. Oberthaler, Rev. Mod. Phys. **78**, 179 (2006).
[17] D. Clément *et al.*, Phys. Rev. Lett. **102**, 155301 (2009).
[18] P. T. Ernst *et al.*, Nature Phys. **6**, 56 (2010).
[19] G. Ritt *et al.*, Phys. Rev. A **74**, 063622 (2006).
[20] T. Salger *et al.*, Phys. Rev. Lett. **99**, 190405 (2007).
[21] G. Cennini *et al.*, Phys. Rev. Lett. **91**, 240408 (2003).
[22] See supplementary material at http://link.aps.org/supplemental/10.1103/PhysRevLett.105.215301 for the experimental method used to realize the Fourier-synthesized optical lattice.
[23] J. Y. Vaishnav and C. W. Clark, Phys. Rev. Lett. **100**, 153002 (2008).
[24] R. Gerritsma *et al.*, Nature (London) **463**, 68 (2010).
[25] M. Kasevich and S. Chu, Phys. Rev. Lett. **67**, 181 (1991).
[26] A. Zenesini *et al.*, Phys. Rev. Lett. **103**, 090403 (2009).
[27] M. Merkl *et al.*, Phys. Rev. Lett. **104**, 073603 (2010).
[28] G. Ferrari *et al.*, Phys. Rev. Lett. **97**, 060402 (2006).